

Long-term Skeletal Muscle Protection After Gene Transfer in a Mouse Model of LGMD-2D

Christina A Pacak^{1,2}, Glenn A Walter^{1,3}, Gabe Gaidosh³, Nathan Bryant³, Melissa A Lewis^{1,2}, Sean Germain^{1,2}, Cathryn S Mah^{1,2,4}, Kevin P Campbell⁵ and Barry J Byrne^{1,2}

¹Powell Gene Therapy Center, University of Florida College of Medicine, Gainesville, Florida, USA; ²Department of Pediatric Cardiology, University of Florida College of Medicine, Gainesville, Florida, USA; ³Department of Physiology, Functional Genomics, University of Florida College of Medicine, Gainesville, Florida, USA; ⁴Department of Cellular, Molecular Therapy, University of Florida College of Medicine, Gainesville, Florida, USA; ⁵HIMI, Department of Physiology, Biophysics, University of Iowa, Iowa City, Iowa, USA

Limb girdle muscular dystrophy (LGMD) describes a group of inherited diseases resulting from mutations in genes encoding proteins involved in maintaining skeletal muscle membrane stability. LGMD type-2D is caused by mutations in alpha-sarcoglycan (*sgca*). Here we describe muscle-specific gene delivery of the human *sgca* gene into dystrophic muscle using an adeno-associated virus 1 (AAV1) capsid and creatine kinase promoter. Delivery of this construct to adult *sgca*^{-/-} mice resulted in localization of the sarcoglycan complex to the sarcolemma and a reduction in muscle fiber damage. *Sgca* expression prevented disease progression as observed *in vivo* by T₂-weighted magnetic resonance imaging (MRI) and confirmed *in vitro* by decreased Evan's blue dye accumulation. The ability of recombinant AAV-mediated gene delivery to restore normal muscle mechanical properties in *sgca*^{-/-} mice was verified by *in vitro* force mechanics on isolated *extensor digitorum longus* (EDL) muscles, with a decrease in passive resistance to stretch as compared with untreated controls. In summary, AAV/AAV-*sgca* gene transfer provides long-term muscle protection from LGMD and can be non-invasively evaluated using magnetic resonance imaging.

Received 4 January 2007; accepted 28 May 2007; published online 24 July 2007. doi:10.1038/sj.mt.6300246

INTRODUCTION

The limb girdle muscular dystrophies (LGMDs) are a group of inherited syndromes characterized by progressive muscle wasting as a result of the breakdown of muscle fiber membrane integrity. Some of these are caused by autosomal dominant mutations, but many forms of LGMD are autosomal recessive disorders caused by mutations in a gene encoding one of the sarcoglycan proteins. The sarcoglycans comprise a complex that consists of a combination of up to six glycosylated transmembrane proteins.¹ This sarcoglycan complex is a small but integral portion of the large dystrophin glycoprotein complex that is vital for maintaining muscle fiber integrity.

The standard care for patients suffering from LGMD-2D is currently aimed at delaying disease progression through low-stress activities; no true treatment is available. For this reason, and because LGMD-2D is the result of a single gene defect, the development of a clinically applicable gene delivery technique combined with non-invasive assessment methods is highly desirable.

Using either adenovirus or the adeno-associated virus (rAAV) gene delivery systems, investigators have demonstrated that providing a correctly functioning form of the *sgca* gene to muscle tissue in a knockout mouse is sufficient to re-establish the dystrophin glycoprotein complex connection to muscle fiber membranes and protect tissue from damage.²⁻⁴ Experiments using adenovirus to deliver the *sgca* gene have demonstrated at least 90% transduction of muscle fibers and an overall decrease in dystrophic lesion formation after a single intra-muscular (IM) injection into neonates.² These studies were important for proving the concept that gene delivery is a potential treatment option for this disease.

rAAV has emerged as a strong candidate for skeletal muscle gene transfer because of its ability to infect non-dividing cells, its ability to persist for long periods, and its proven safety *in vivo*.⁵⁻¹⁰ It has been shown that delivery of the *sgca* gene using rAAV serotype 2 (rAAV2) results in alpha-sarcoglycan expression and successful localization of the entire sarcoglycan complex to the myofiber membranes.³ It was observed that between 28 and 41 days after injection a dramatic decrease in *sgca* expression occurred in these muscles. Further analysis indicated that this was believed to be the result of *sgca* over-expression using a CMV promoter.³ These studies revealed that a fine balance exists in the protein expression within myofibers, which must be maintained to achieve functionally corrective expression levels of alpha-sarcoglycan and concurrently avoid the elicitation of an immune response and subsequent negative consequences. Here we describe a series of experiments that have achieved this balance through the use of a construct that exploits the rAAV1 capsid in combination with a truncated creatine kinase-based muscle-specific promoter to achieve a physiologically more accurate level of *sgca* expression.

Correspondence: Barry J. Byrne, Powell Gene Therapy Center, University of Florida College of Medicine, 1600 SW Archer Road, ARB RG-183, Gainesville, Florida 32610, USA. E-mail: bbyrne@ufl.edu

We hypothesized that the use of an rAAV1/2 pseudotype containing a truncated creatine kinase promoter would result in early muscle-specific expression of human *sgca*, achieving sufficient amounts of *sgca* protein to maintain cell membrane integrity without eliciting an immune response. Furthermore, the effect of *sgca* expression on function and morphology would be corrective and prevent disease progression in both adult and newborn *sgca*^{-/-} mice. To test this hypothesis, functional correction was determined using *in vitro* force mechanics and histological analysis was performed on tissue sections. In addition, magnetic resonance imaging (MRI) was used to monitor dystrophic lesion development over time non-invasively. In lieu of human clinical trials for this therapy, there is a great need for a non-invasive, quantitative assessment technique to establish efficacy.

RESULTS

In vitro *sgca* gene expression

Infection of differentiated primary *sgca*^{-/-} myotubes with the rAAV2/1-tMCK-*sgca* viral construct results in the expression of *sgca*. Myoblasts were isolated from *sgca*^{-/-} neonates and forced into differentiation using previously described methods.¹¹ Once fully differentiated, the *sgca*^{-/-} myotubes were infected with rAAV2/1-tMCK-*sgca* at a multiplicity of infection of 10,000 (Figure 1a). An anti-desmin antibody was used to show myoblast differentiation (red), and *sgca* protein (green) was detected after infection by immunofluorescence and by western blot analysis (data not shown).

Sgca gene delivery to adult *sgca*^{-/-} mice

Histopathological signs associated with LGMD were reduced 2 months after IM injection of 1×10^{11} vector genomes (vg) of rAAV2/1-tMCK-*sgca* in adult *sgca*^{-/-} *tibialis anterior* and *extensor digitorum longus* (EDL) muscles. *In vitro* tissue analysis revealed that treated legs displayed numerous *sgca*⁺ muscle fibers and improved morphology compared with untreated contra-lateral hindlimb muscles in terms of both decreased membrane permeability [determined by the number of Evans blue dye (EBD)-positive fibers] and decreased fibrosis in areas expressing *sgca* (Figure 1b; upper panels).

A second cohort of animals showed continued tissue correction 6 months after vector administration. Immunofluorescence analysis revealed that only those muscles injected with the rAAV2/1-tMCK-*sgca* construct expressed *sgca*, and those located in the uninjected contra-lateral hindlimb displayed a notable increase in the number of EBD-positive muscle fibers and areas with fibrosis (Figure 1b; lower panels).

Functional correction in *sgca*^{-/-} mice treated as adults

A passive resistance to stretch protocol was performed on EDL muscles from both treated and untreated hindlimbs of *sgca*^{-/-} mice at 6 months after injection. rAAV2/1-tMCK-*sgca*-injected muscles were found to have a resistance to passive stretch of 5.24 ± 2.12 g/cm² and were similar to healthy age-matched B6/129 EDL muscles (8.53 ± 0.67 g/cm²; *P*-value = 0.32; Figure 2). Untreated *sgca*^{-/-} EDL muscles fell into two distinct categories: those generating an abnormally low resistance to passive stretch (1.56 ± 0.29 g/cm²; *P*-value = 0.0001) and those demonstrating an

abnormally high resistance to passive stretch (17.03 ± 2.59 g/cm²; *P*-value = 0.04) compared with age-matched controls. A relationship between high resistance to stretch and fibrosis was observed in one group (fibrotic lesions), and the second group displayed a correlation between low resistance to passive stretch and the number of EBD-positive fibers (EBD lesions). Analysis of tissue sections by blinded observers revealed that on average 66% of all EDL fibers were expressing the *sgca* gene in treated muscles. Low levels of EBD infiltration and no fibrosis were observed in cryosections of *sgca*-expressing muscles at either 2 or 6 months after vector administration.

IM delivery to newborn *sgca*^{-/-} mice

We determined the effect of rAAV2/1-tMCK-*sgca* administered before the onset of lesion development using a method that

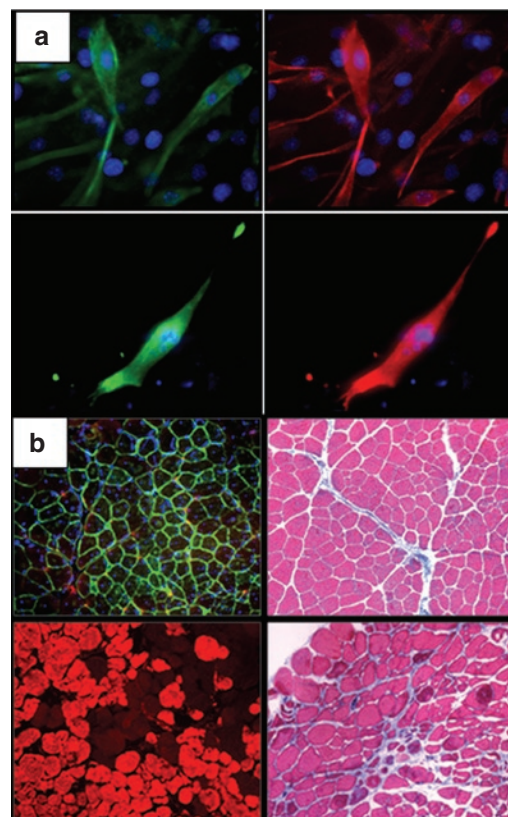


Figure 1 Expression in primary alpha-sarcoglycan (*sgca*)^{-/-} myoblasts and adult treated mice. **(a)** Differentiated C2C12 myoblasts (top two panels) display *sgca* protein expression (green) as well as desmin expression (red). Differentiated primary *sgca*^{-/-} myoblasts (bottom two panels) infected with rAAV2/1-tMCK-*sgca* at a multiplicity of infection of 10,000 show *sgca* expression (green). **(b)** Immunofluorescence and trichrome stain (top two panels) images from frozen tissue sections 2 months after administration of the rAAV2/1-tMCK-*sgca* construct (1×10^{11} vector genomes per mouse) performed as a deep injection along the tibia into left *tibialis anterior* (TA) and *extensor digitorum longus* (EDL) lower hindlimb muscles of 2-month-old *sgca*^{-/-} mice. (Top left panel) *sgca* expression (green) in TA muscle injected with rAAV2/1-tMCK-*sgca* and Evans blue dye (EBD) before mice were killed. No EBD infiltration is observed in myofibers expressing *sgca*. (Top right panel) Trichrome-stained section from the same muscle. (Bottom left panel) No *sgca* expression (no green) in an uninjected contra-lateral TA muscle. EBD infiltration is evident in red. (Bottom right panel) Trichrome-stained tissue section from the same uninjected muscle displays evidence of fibrosis and collagen infiltration.

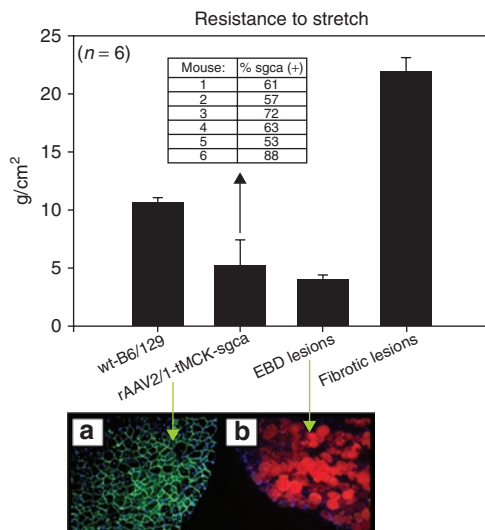


Figure 2 Resistance to passive stretch force mechanics on *extensor digitorum longus* (EDL) muscles from mice injected with rAAV2/1-tMCK-*sgca*, wild-type controls, and uninjected *sgca*^{-/-} mice ($n = 6$ per group). Untreated *sgca*^{-/-} muscles fell into two distinct groups: those with clear evidence of Evans blue dye (EBD) uptake (displaying a low resistance to stretch) and those showing signs of fibrosis as determined by the trichrome stain for collagen infiltration (displaying a high resistance to stretch). **(a)** Example of treated EDL expressing *sgca* (green). **(b)** Example of an EBD-infiltrated untreated EDL. All EDL muscles from rAAV2/1-tMCK-*sgca*-treated legs demonstrated the presence of *sgca* protein by immunohistological staining in at least 50% of myofibers. *sgca*, alpha-sarcoglycan.

achieves wide vector distribution and its effect on the formation of dystrophic lesions. One-day-old *sgca*^{-/-} neonates ($n = 6$) were injected with 1×10^{11} vg of rAAV2/1-tMCK-*sgca* in one hindlimb (IM, total volume 35 μ l) and 1×10^{11} vg of rAAV2/1-tMCK-*LacZ* in the contra-lateral hindlimb (single injection per leg). The contra-lateral mock injections were necessary to control for the potential effect of muscle repair mechanisms being triggered through the physical act of needle administration into muscle. We observed no such corrective or damage-preventing affect when the rAAV2/1-tMCK-*LacZ*-injected *sgca*^{-/-} muscles were compared with uninjected, untreated *sgca*^{-/-} muscles.

MRI technique for assessing damaged muscle tissue

Areas of muscle damage were determined non-invasively using MRI. The hindlimbs of injected mice were imaged using a single tuned solenoid coil and T₂-weighted MRI beginning at 4 weeks of age (4 weeks after injection). Twelve diffusion-controlled T₂-weighted images were acquired (from ankle to knee) to calculate the total damaged area in each hindlimb (**Figure 3**).^{12,13} The image pixels with an elevated T₂ non-invasively identified the volume of dystrophic lesion development in each hindlimb over 3-week intervals throughout the course of the experiment (**Figure 3a** and **b**). The two-dimensional images displayed correspond to the maximal cross-sectional area of the lower hindlimb (slice 9 or 10 from sets of 12 images beginning at the ankle and ending at the knee). When considered as a group, the affected tissue volumes within the untreated hindlimbs were significantly (P -value ≤ 0.001) higher than those observed within either rAAV2/1-tMCK-*sgca*-treated hindlimbs or healthy age-matched controls that

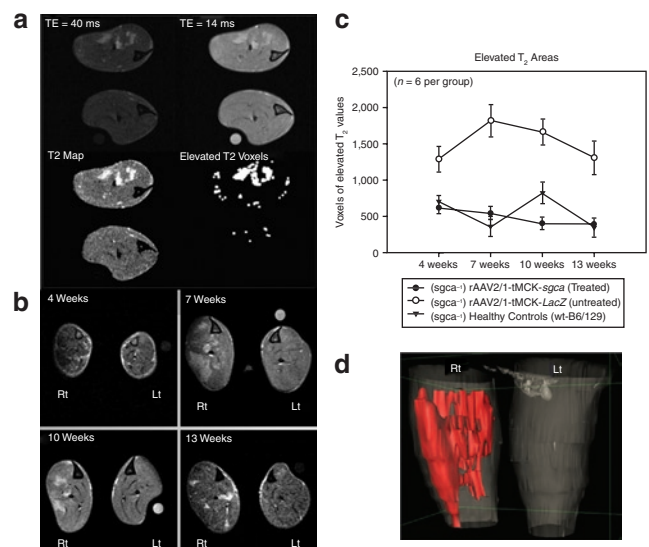


Figure 3 Non-invasive T₂ mapping data for damaged tissue were determined non-invasively by quantitative processing of T₂-weighted magnetic resonance (MR) images.^{14,15} **(a)** A T₂ map (bottom left panel) is derived from information provided by a combination of 14- and 40-ms echo-time (TE) scans (top panels). Using this T₂ map, a threshold value is set for the average signal intensity of healthy muscle tissue and each voxel is scored as elevated or normal. A binary image is created of voxels with elevated T₂s (bottom right panel) that are then quantified. Images are at 10 weeks of age. **(b)** MR images from one *sgca*^{-/-} mouse at 4, 7, 10, and 13 weeks after administration of the rAAV2/1-tMCK-*sgca* construct [1×10^{11} vector genomes (vg)] into the left leg and the rAAV2/1-tMCK-*LacZ* construct (1×10^{11} vg) into the right leg as a 1-day-old neonate. Images presented are cross-sectional slices of each pair of hindlimbs at their widest level (slice 9 or 10 from sets of 12 images beginning at the ankle and ending at the knee). A total of 72 slices were assessed for each group of mice at each time point (6 mice, 12 slices each). Dystrophic lesions developing over time appear as areas of higher than normal signal intensity and are apparent in the right (untreated, mock-injected) leg and absent in the left (treated) leg. **(c)** A graphical representation of the time course for dystrophic lesion development as observed by non-invasive MRI T₂ analysis in untreated *sgca*^{-/-} hindlimbs, and the lack thereof in age-matched treated *sgca*^{-/-} and wild-type mouse hindlimbs. **(d)** A three-dimensional rendering of regions of elevated T₂ (pseudocolored red) based on multi-slice T₂-weighted MR images from the hindlimbs (pseudocolored blue) of a *sgca*^{-/-} mouse with one leg expressing alpha-sarcoglycan.

showed similar results throughout the duration of this experiment (**Figure 3c**). The relatively small number of elevated voxels detected in healthy hindlimbs are indicative of partial volume effects from subcutaneous fat. A three-dimensional rendering of pixels with elevated T₂ (shown in red in **Figure 3d**) based on the multi-slice T₂ images of both mouse hindlimbs (in blue) is shown in **Figure 3d** and demonstrates the extent of lesion development throughout the muscles of the right lower hindlimb and the lack of damage in the left (treated) lower hindlimb (**Figure 3d**).

sgca expression and tissue analysis of newborn treated mice

EBD analysis [both bright-field (blue) and epifluorescence (red)] of excised whole muscles from these mice clearly confirmed what was observed using the MRI T₂ technique: muscles from untreated hindlimbs accumulated EBD and muscles from the treated contra-lateral hindlimbs did not (**Figure 4a** and **b**) ($n = 6$). Cryosection analysis showed that all muscles from the hindlimbs injected with

the rAAV2/1-tMCK-*sgca* construct were expressing *sgca* and those muscles from the contra-lateral hindlimbs had no expressions (Figure 4f and i). On average, 79% of treated EDL muscle fibers displayed *sgca* expression. The control injected hindlimbs displayed widespread expression of *LacZ* in some areas (data not shown), whereas other areas, which corresponded to fibrosis, completely lacked expression. This lack of expression is most likely due to loss of vector-containing muscle fibers as a result of lesion formation and subsequent cell degradation.

Serial sections from these muscles were also stained for the gamma-sarcoglycan (sgcg) protein (Figure 4d, g, and j). As expected, sgcg was observed only in those fibers in which the *sgca* protein was present. This indicated that in the presence of *sgca*, other components of the sarcoglycan complex were able to migrate to their normal position at the sarcolemma. We did not observe EBD infiltration in areas where *sgca* protein was present, suggesting that a fully functional dystrophin glycoprotein complex in the membrane was providing those muscle fibers protection from lesion development.

Passive stretch analysis of neonatally treated mice

Neonatally treated muscles developed neither the tendency to display an abnormally low resistance to passive stretch (indicative of early-stage lesion development; $3.15 \pm 0.38 \text{ g/cm}^2$) nor the abnormally high resistance to passive stretch (indicative of late-stage lesion development; $17.46 \pm 1.02 \text{ g/cm}^2$) that was observed in age-matched, untreated, or mock-injected control EDL muscles (Figure 4l). The resistance to stretch of healthy age-matched (4-month-old) wild-type control muscles was $8.53 \pm 0.34 \text{ g/cm}^2$ and that of rAAV2/1-tMCK-*sgca*-treated muscles was similar at $7.00 \pm 0.61 \text{ g/cm}^2$ ($n = 6$); these results were significantly different from those for untreated fibrotic muscles (P -value = 0.007). This demonstrated that early treatment not only preserves muscle fiber integrity, as demonstrated by MRI and EBD analysis, but also provides preservation of mechanical function in those muscles expressing *sgca*.

Long-term expressions 1 year after neonatal administration

Longevity of expression and subsequent prevention of the disease phenotype was evident out to 1 year after administration of rAAV2/1-tMCK-*sgca*. One-day-old *sgca*^{-/-} neonates ($n = 4$) were injected with 1×10^{11} vg of rAAV2/1-tMCK-*sgca* in one hindlimb (IM, total volume 35 μl) and 1×10^{11} vg of rAAV2/1-tMCK-*LacZ* in the contra-lateral hindlimb (single injection per leg). Tissues were harvested 1 year after injection. Analysis of excised muscles using bright field and epifluorescence demonstrated little to no EBD uptake in treated legs as compared with *LacZ*-injected controls (Figure 5a and b). Tension generation during a passive stretch showed a significant difference (P -value = 0.032) between the resistance to stretch displayed by treated EDL muscles and that displayed by untreated controls, with untreated muscles showing a resistance threefold greater than that observed in age-matched, healthy B6/129 EDL muscles (Figure 5c). At this 1-year time point all untreated *sgca*^{-/-} muscles had an increased resistance to stretch, indicative of these tissues undergoing late-stage lesion development and fibrosis. Histological analysis of cryosections

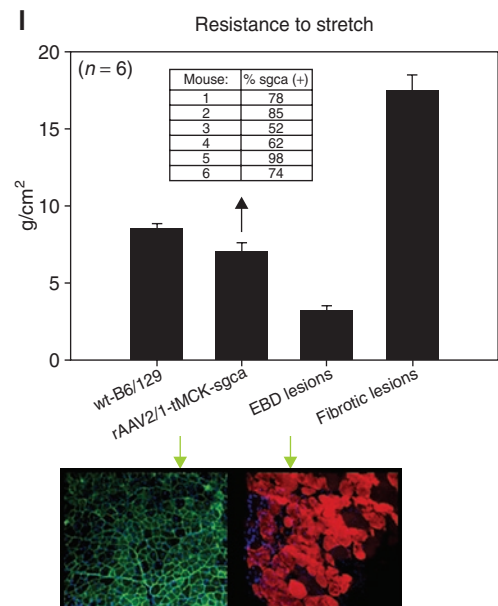
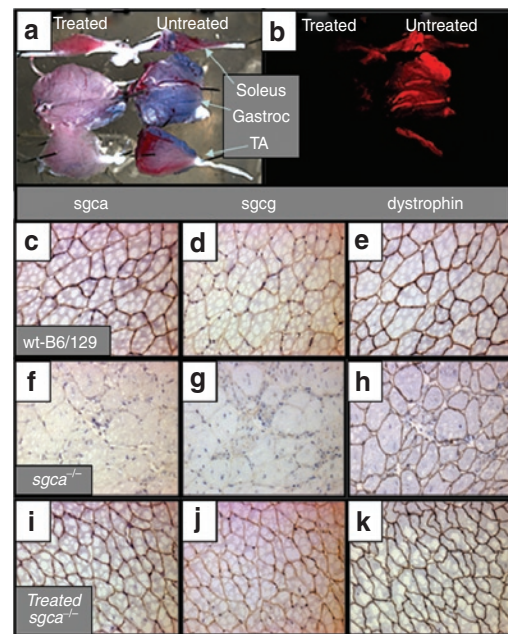


Figure 4 Functional and morphological analysis of muscles from neonatally treated mice. (a) Bright-field image of excised muscles from the lower hindlimbs. From top to bottom: *extensor digitorum longus* (EDL), *gastrocnemius* (Gastroc), *tibialis anterior* (TA). Muscles in the left column are from the rAAV2/1-tMCK-*sgca*-injected hindlimb [where little to no Evans blue dye (EBD) infiltration is observed (blue)], and the right-column muscles are from the rAAV2/1-tMCK-*LacZ*-injected hindlimb. (b) Image of the same muscles under Texas Red fluorescence (EBD fluoresces red). Serial tissue sections from TA muscles of age-matched (c–e) wild-type, (f–h) *sgca*^{-/-}, and (i–k) treated *sgca*^{-/-} mice showing antibody staining of alpha-sarcoglycan (sgca) (c, f, i), gamma-sarcoglycan (sgcg) (d, g, j), and dystrophin (e, h, k). (l) Passive stretch force mechanics on EDL muscles from mice injected with rAAV2/1-tMCK-*sgca*, wild-type controls, and uninjected *sgca*^{-/-} mice ($n = 6$ per group) at 3 months of age (3 months after injection). Arrows point to an example of a treated EDL and an EBD-infiltrated untreated EDL. Resistance to stretch of treated *sgca*^{-/-} EDL muscles is comparable to that of healthy age-matched wild-type controls. All EDL muscles from rAAV2/1-tMCK-*sgca*-treated legs demonstrated the presence of *sgca* protein by immunohistological staining in at least 50% of myofibers.

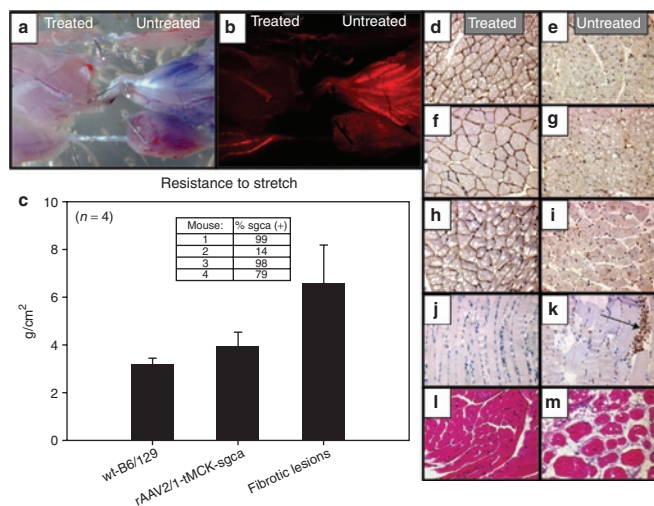


Figure 5 Functional and morphological analysis of muscles from mice treated at 1 day of age at 1 year after vector administration. **(a)** From top to bottom: *extensor digitorum longus* (EDL), *gastrocnemius* (Gastroc), *tibialis anterior* (TA). Muscles in the left column are from the rAAV2/1-tMCK-*sgca*-injected hindlimb [where little to no Evans blue dye (EBD) infiltration is observed (blue)], and the right-column muscles are from the rAAV2/1-tMCK-*LacZ*-injected hindlimb. **(b)** Image of the same muscles under Texas Red fluorescence (EBD fluoresces red). **(c)** Passive stretch force mechanics on EDL muscles from mice injected with rAAV2/1-tMCK-*sgca*, wild-type controls, and uninjected *sgca*^{-/-} mice ($n = 4$ per group) at 1 year of age (1 year after injection). Resistance to stretch of treated *sgca*^{-/-} EDL muscles is comparable to that of healthy age-matched wild-type controls and lower than that of untreated *sgca*^{-/-} EDL muscles, indicating they are less fibrotic. **(d–i)** Skeletal muscle sections (EDL, TA, and Gastroc) from treated **(d, f, h)** and untreated **(e, g, i)** hindlimb muscles stained with alpha-sarcoglycan antibody. **(j)** Treated and **(k)** untreated skeletal muscle sections stained for the caspase 3 apoptosis marker. Arrow indicates caspase 3 staining in untreated gastroc. **(l)** Treated and **(m)** untreated gastroc showing excessive fibrosis in untreated muscle.

showed that on average 73% of EDL muscle fibers from rAAV2/1-tMCK-*sgca* hindlimbs displayed *sgca* protein expression 1-year after administration (Figure 5d). Antibody staining of cryosections also identified *sgca* expression in the gastroc and *tibialis anterior* muscles of treated hindlimbs but not in the contra-lateral hindlimbs (Figure 5f–i).

Another hallmark of dystrophic muscle fibers is their tendency to display centralized nuclei. The presence of centralized nuclei is often associated with muscle fiber regeneration, along with fiber size variations, fiber necrosis, and fiber atrophy¹⁴ and has been previously described in this model.¹⁵ In the current studies we did not observe the reversal of this phenotype when rAAV2/1-tMCK-*sgca* was administered to adult *sgca*^{-/-} mice. On the other hand, histological analysis of muscles injected at 1 day of age showed that we did successfully prevent this from occurring in those muscles treated before the onset of lesion development. Blinded analysis of EDL muscle sections from six treated and six untreated hindlimbs at 1 year after rAAV2/1-tMCK-*sgca* administration revealed that 2% of the muscle fibers expressing *sgca* displayed centralized nuclei, whereas 100% of fibers not expressing *sgca* displayed centralized nuclei.

Finally, we performed a caspase 3 stain on cryosections from muscles of treated and mock-injected hindlimbs. Analysis of

tissue sections from our experiments showed that caspase 3 was apparent only in areas of extremely late-stage lesion development where fibrosis and deterioration of muscle fibers had previously occurred; it was not found in treated muscles (Figure 5j–m).

DISCUSSION

The overall aim of this study was to determine whether disease progression can be prevented in a mouse model of LGMD-2D using an AAV-mediated gene delivery technique. We found that the expression of *sgca* prevented disease progression, as observed *in vivo* by MRI T₂ assays and three-dimensional image reconstruction. This outcome was confirmed *in vitro* by a decrease in Evan's blue dye accumulation, trichrome staining, and immunohistochemistry. The ability of rAAV2/1-mediated gene delivery to restore normal mechanical properties in *sgca*^{-/-} mice was verified by *in vitro* force mechanics on isolated EDL muscles. Moreover, we found that the use of a muscle-specific promoter and the AAV2/1-pseudotyped vector provides long-term expression of *sgca* and results in protection of skeletal muscle integrity in *sgca*^{-/-} mice for up to at least 1 year after vector administration. This lends further support to a recent study by Fougere et al. that demonstrated similar success using an intra-arterial delivery method.¹⁶

The expression of *sgca* lasts for up to 6 months after injection following delivery of our rAAV2/1-tMCK-*sgca* construct to adult *sgca*^{-/-} mice and up to at least 1 year following a single IM injection in 1-day-old neonates. Although some amount of disease correction following adult administration was observed, prevention of the typical disease phenotypes (lesion development, resistance to stretch, and tissue fibrosis) was achieved following vector administration at the earlier, 1-day-old time point.

In measuring the resistance to stretch of treated and untreated *sgca*^{-/-} muscles and comparing them to results for age-matched wild-type controls, we found that whereas early treatment resulted in correction of this phenotype to wild-type levels, treatment in adult muscle tissue attenuated the phenotype to approximately 50% wild-type values. Our histological analyses of gene delivery to neonatal and adult tissues suggest that there is a window of opportunity during disease progression when a muscle fiber can still be protected. Beyond this point the muscle has progressed too far down the cascade of tissue damage for recovery or even the ability to halt further damage.

Our observation that the passive stretch performance of EDL muscles from untreated *sgca*^{-/-} animals fell into two categories early on—high and low (resistance to stretch), corresponding to EBD lesion formation and fibrosis (respectively)—and only one category by a year of age—high resistance to stretch—suggests a model for the progression of muscle wasting and fibrosis in this disease. The early-stage lesions (deemed so by EBD infiltration and/or MRI T₂ assessment) are indicative of decreased sarcolemmal integrity. These fragile membranes operating with inadequate dystrophin-glycoprotein complexes are then unable to perform their proper force modulation functions, including providing stretch resistance. On the basis of our findings, once the myofiber reaches this state it is destined to proceed down a pathway of destruction that includes collagen infiltration and fibrosis in the later stages. The passive stretch data reported here demonstrate

the relative inflexibility of EDL muscles comprised of collagenous fibers as compared with the healthy normal or treated EDL muscles in which membrane stability was maintained.

One of the many difficulties in designing a therapeutic approach to a disorder such as LGMD-2D is the progressive nature of these types of diseases. It would therefore be ideal to initiate gene delivery immediately upon diagnosis in the clinical setting to halt further disease progression and maintain an overall higher quality of life for patients.

An additional challenge to designing a gene delivery approach for the dystrophies is that many of the affected proteins are membrane bound and not secreted. When delivering genes encoding secreted proteins, one has the potential advantage of using the injected muscle as a depot or factory for producing sufficient amounts of protein to be secreted and distributed throughout the entire body.¹⁷ Because the *sgca* protein is not secreted, the viral gene delivery vehicle must transduce each individual fiber in which expression is desired for that muscle cell to display the protein. Our passive stretch analyses indicates that transduction of at least 50% of muscle fibers in the EDL was sufficient to provide protection of that particular muscle from the typical resistance to stretch that develops as dystrophic lesions progress from “leaky” muscle fibers into areas of fibrotic collagen. This confirms that complete transduction of every cell in a tissue is not required for successful protection of skeletal muscle.

Caspase 3 is one of many proteases that mediate the execution of apoptosis, or the intrinsic suicide mechanism by which cells destroy themselves. Stained tissue sections showed caspase 3 expression in only a few areas of severe fibrosis in muscles from untreated hindlimbs; it was not observed in any of the treated muscles.

We chose to perform MRI assessment for detection of areas of damaged tissue (dystrophic lesion development) at 3-week intervals beginning at 4 weeks of age and ending at 13 weeks of age. Tissue section analysis in a preliminary experiment showed that no EBD uptake occurs until this time point. This is therefore a critical developmental window when the onset of dystrophic lesion growth occurs owing to muscle damage and MRI can be most easily used to detect these areas owing to shifts in water compartmentalization. Fibrosis progresses as the mouse ages, and the infiltration of collagen into damaged areas may reduce the ability of this particular MRI technique to identify those late-stage fibrotic lesions owing to the ultrashort T_2 associated with collagen. Other MRI techniques that rely on magnetization transfer or differences in apparent diffusion of water and metabolites may provide additional information in fibrotic tissues to complement the T_2 measurement.

In comparison to extraction of muscle biopsies, the use of MRI for non-invasive analysis of skeletal muscle integrity is an attractive method for assessing the success of any therapy aimed at preventing the progression of muscular dystrophy. Here we implement a recently developed T_2 mapping method to identify areas of tissue damage as a result of dystrophic lesion development within skeletal muscle. This technique can be easily applied to humans and used for analysis of other muscular dystrophies or diseases in which the integrity of muscle fiber membranes is compromised, allowing for excess water, albumin, or serum proteins

to occur. Importantly, to differentiate between muscles that were corrected after AAV delivery of *sgca* and those in which the disease was allowed to progress, the injection of a contrast reagent was not required. These studies clearly demonstrate the ability of this method to provide *in vivo* monitoring of the beneficial effects of therapeutic vector delivery to *sgca*^{-/-} knockout muscle tissue.

In conclusion, we have developed an AAV2/1-mediated gene delivery system that demonstrates successful prevention of the LGMD-2D phenotype when delivered at an early age in a mouse model of the disease. This construct is also able to protect adult tissue from further damage when delivered at a later time point. In addition, we have demonstrated the application of a non-invasive, MRI-based T_2 mapping technique to monitor the development of dystrophic lesions over time (or lack thereof) *in vivo*. The results of these studies indicate that further investigation of these techniques is warranted in human patients suffering from LGMD-2D.

MATERIALS AND METHODS

rAAV construct and virus preparation. The creatine kinase-based promoter described in this text (tMCK) was a kind gift from Dr. Xiao Xiao (University of Pittsburg, PA). The sequence is:

```
gcttctgatacctcgagatctgaattcgagctgcatgccactacgggtctaggctgccatgta
aggaggcaaggcctggggacacccgagatgctggttataattaacccaacacct
gctgcccccccccaacacctgctgctgagctgagcggttacccccgggtgctggg
tcttaggctctgtacacatggaggagaagctgctctaaaaataacctgtcctgggtgac
cactacgggtctaggctgccatgtaaggaggcaaggcctggggacacccgagatgctggtt
aattaacccaacacctgctgcccccccccaacacctgctgctgagcctgagcgggtacc
ccacccgggtgctgggtcttaggctctgtacacatggaggagaagctgctctaaaaa
taacctgtcctgggtgacacactacgggtctaggctgccccatgtaaggaggcaaggc
ctggggacacccgagatgctggttataattaacccaacacctgctgcccccccccaac
acctgctgctgagcctgagcggttacccccgggtgctggtgctttaggctctgt
acacatggaggagaagctgctctaaaaataacctgtcctgggtgacacacccgggga
cagccccctctgctagtcacacctgtaggctcctctataacccaggggacaggggctg
ccccgggtcactcgagaggcctaataagagctcagatgcatgcatgagtggtggtt
ttgtgtgagatctgacctgacg. It is a modification of the previously described
CK6 promoter18 and contains a triple E box sequence. Both the rAAV1 and
rAAV2 viruses used in these experiments were prepared by the University
of Florida Vector Core Facility using a previously described plasmid trans-
fection technique.19 The sgca sequence used in this vector is the human
complementary DNA U08895 (1404 base pairs) placed in the pTR-UFG
backbone.20,21
```

Knockout mouse model. The *sgca*^{-/-} mouse model used in these studies was developed by Dr. Kevin Campbell (University of Iowa).¹⁵ These mice display progressive muscular dystrophy in the form of dystrophic lesion formation, fibrosis, apoptosis, and skeletal muscle stiffness as measured through passive stretch force mechanics analysis over a lifespan of approximately 18 months.¹⁵

Immunofluorescence antibody staining. Immunofluorescence staining was performed on unfixed cryosections. In brief, sections were first rinsed in phosphate-buffered saline for 5 minutes at room temperature. They were then placed in 3% bovine serum albumin blocker for 20 minutes at room temperature. Primary *sgca* antibody (provided by Kevin Campbell, University of Iowa) was diluted 1:15 and placed on sections overnight at 4°C. Sections were then rinsed in phosphate-buffered saline two times for 5 minutes each followed by secondary antibody incubation for 20 minutes. Sections were again rinsed with phosphate-buffered saline then mounted on a glass coverslip using 4',6-diamidino-2-phenylindole mounting medium (Vector Laboratories, Burlingame, CA). All tissue sections were assessed for *sgca* expression by blind analysis. *sgca*⁺ myofibers were divided by total number of nuclei to determine percentage expression.

Trichrome and immunohistochemical staining. Trichrome staining was performed according to instructions provided with the Masson Trichrome Stain Kit (Richard-Allan Scientific, Kalamazoo, MI, procedure number 010, catalogue number 87010). Immunohistochemical staining was performed by the University of Florida Molecular and Pathology Core facility on paraffin-embedded tissue sections using provided protocols for the caspase 3 rabbit polyclonal antibody (Biocare Medical, Concord, CA; catalogue number CP229A) and the alpha-sarcoglycan mouse monoclonal antibody (Novocastra Laboratories, Newcastle upon Tyne, UK; catalogue number NCL-a-SARC). All tissue sections were assessed for fibrosis and apoptosis by blinded readers.

sgca^{-/-} IM injections. All animal procedures were performed according to University of Florida Institutional Animal Care and Use Committee guidelines. Adult IM injections were performed by anesthetizing 2-month-old sgca^{-/-} mice under a mixture of 1.5% isoflurane and O₂ (1–2 l). One-day-old sgca^{-/-} mice were anesthetized by induced hypothermia. For adults, the area of the lower hindlimb was cleaned and depilatory cream was used to remove fur. A 29.5-G tuberculin syringe was used to perform single IM injections of each vector diluted in phosphate-buffered saline (total volume of 35 µl per injection) into 1-day-old neonate and adult legs. The needle point was inserted near the bundle of tendons at the ankle and pointing up into the *tibialis anterior* along the tibia to the knee for adult hindlimbs and into quadriceps area for neonate injections. For both adult and 1-day-old neonate injections the virus solution was injected while withdrawing the needle to maximize volume distribution.

Non-invasive MRI T₂ assessment. MRI experiments were performed as previously described.^{12,13} In brief, each mouse was sedated with a mixture of 1.5% isoflurane and O₂ (1–2 l) ($n = 6$ per group, per time point). The lower hindlimbs were aligned next to one another, positioned inside a five-turn, 1.5-cm inner diameter, single-tuned proton solenoid coil, and MR imaged using a 4.7-tesla Bruker Avance spectrometer. After an initial positioning scan, multiple-slice, diffusion controlled, single spin-echo images were acquired with the following parameters: pulse repetition time, 2,000 ms; echo times, 14 and 40 ms; field of view, 10–20 mm; slice thickness, 0.5–1.0 mm; acquisition matrix size, 256 × 128; diffusion weighting, 3 mm²/s, and two signal averages. To avoid the contribution of stimulated echoes to the T₂ measurement, we implemented a Hahn spin-echo MR image sequence in which two separate acquisitions were acquired at echo times of 14 and 40 ms. T₂ maps and volumes of elevated T₂s were determined using custom software (Interactive Data Language; ITT Industries, Boulder, Co; RSI, Boulder, CO). Three-dimensional data were rendered using Osirix Dicom viewing software (<http://homepage.mac.com/rossetantoinne/osirix/>). Statistics were calculated using a Student's *t*-test.

Force mechanics. All resistance to force mechanics measurements were performed *in vitro* as previously described.^{22–24} In brief, EDL muscles were tied to a force transducer at full length (L₀). Each muscle was extended to 110% L₀ then allowed to relax, and resistance to stretch was measured. The passive stretch experiment was performed three times per muscle and resistances were averaged. Statistics were calculated using a Student's *t*-test.

ACKNOWLEDGMENTS

We would like to thank the University of Florida Viral Vector Core for making the virus preparations used in these experiments. Also we would like to acknowledge the University of Florida Advanced Magnetic Resonance Imaging and Spectroscopy Facility for their assistance in the MRI described in this work and the Molecular

Pathology and Immunology Core for tissue section preparations. This work was supported by grants from the National Institutes of Health (NHLBI PO1 HL59412, NIDDK PO1 DK58327, AT-NHLBI-U01 HL69748, AR47292 and Glenn A. Walter was supported by RO1 HL78670), the Muscular Dystrophy Association, and the American Heart Association (AHA) Florida and Puerto Rico Affiliate (C.A.P.) and the National Center of the AHA (C.S.M.). B.J.B., the Johns Hopkins University, and the University of Florida could be entitled to patent royalties for inventions described in this manuscript.

REFERENCES

- Moore, SA, Shilling, CJ, Westra, S, Wall, C, Wicklund, MP, Stolle, C *et al.* (2006). Limb-girdle muscular dystrophy in the United States. *J Neuropathol Exp Neurol* **65**: 995–1003.
- Allamand, V, Donahue, KM, Straub, V, Davison, RL, Davidson, BL and Campbell KP (2000). Early adenovirus-mediated gene transfer effectively prevents muscular dystrophy in alpha-sarcoglycan-deficient mice. *Gene Ther* **7**: 1385–91.
- Dressman, D, Araishi, K, Imamura, M, Sasaoka, T, Liu, LA, Engvall, E *et al.* (2002). Delivery of alpha- and beta-sarcoglycan by recombinant adeno-associated virus: efficient rescue of muscle, but differential toxicity. *Hum Gene Ther* **13**: 1631–1646.
- Stedman, H, Wilson, JM, Finke, R, Kleckner, AL and Mendell, J (2000). Phase I clinical trial utilizing gene therapy for limb girdle muscular dystrophy: alpha-, beta-, gamma-, or delta-sarcoglycan gene delivered with intramuscular instillations of adeno-associated vectors. *Hum Gene Ther* **11**: 777–790.
- Carter, BJ, Khoury, G and Denhardt, DT (1975). Physical map and strand polarity of specific fragments of adenovirus-associated virus DNA produced by endonuclease R-EcoRI. *J Virol* **16**: 559–568.
- Clark, KR, Sferra, TJ and Johnson, PR (1997). Recombinant adeno-associated viral vectors mediate long-term transgene expression in muscle. *Hum Gene Ther* **8**: 659–669.
- Kessler, PD, Podsakoff, GM, Chen, X, McQuiston, SA, Colosi, PC, Matelis, LA *et al.* (1996). Gene delivery to skeletal muscle results in sustained expression and systemic delivery of a therapeutic protein. *Proc Natl Acad Sci USA* **93**: 14082–14087.
- Podsakoff, G, Wong, KK and Chatterjee S (1994). Efficient gene transfer into nondividing cells by adeno-associated virus-based vectors. *J Virol* **68**: 5656–5666.
- Srivastava, A, Lusby, EW and Berns, KI (1983). Nucleotide sequence and organization of the adeno-associated virus 2 genome. *J Virol* **45**: 555–564.
- Xiao, X, Li, J and Samulski, RJ (1996). Efficient long-term gene transfer into muscle tissue of immunocompetent mice by adeno-associated virus vector. *J Virol* **70**: 8098–8108.
- Blau, HM and Webster, C (1981). Isolation and characterization of human muscle cells. *Proc Natl Acad Sci USA* **78**: 5623–5627.
- Frimel, TN, Walter, GA, Gibbs, JD, Gaidosh, GS and Vandenberg, K (2005). Noninvasive monitoring of muscle damage during reloading following limb disuse. *Muscle Nerve* **32**: 605–612.
- Walter, G, Cordier, L, Bloy, D and Sweeney, HL (2005). Noninvasive monitoring of gene correction in dystrophic muscle. *Magn Reson Med* **54**: 1369–1376.
- Vladutiu, GD and Idiculla, S (1997). Association between internalized nuclei and mitochondrial enzyme defects in muscle. *Muscle Nerve* **20**: 760–763.
- Duclos, F, Straub, V, Moore, SA, Venzke, DP, Hrsta, RF, Crosbie, RH *et al.* (1998). Progressive muscular dystrophy in alpha-sarcoglycan-deficient mice. *J Cell Biol* **142**: 1461–1471.
- Fougerousse, F, Bartoli, M, Poupiot, J, Arandel, L, Durand, M, Guerchet, N *et al.* (2007). Phenotypic Correction of alpha-Sarcoglycan Deficiency by Intra-arterial Injection of a Muscle-specific Serotype 1 rAAV Vector. *Mol Ther* **15**: 53–61.
- Fraites, TJ Jr, Schleissing, MR, Shanely, RA, Walter, GA, Cloutier, DA, Zolotukhin, I *et al.* (2002). Correction of the enzymatic and functional deficits in a model of Pompe disease using adeno-associated virus vectors. *Mol Ther* **5**: 571–578.
- Shield, MA, Haugen, HS, Clegg, CH and Hauschka, SD (1996). E-box sites and a proximal regulatory region of the muscle creatine kinase gene differentially regulate expression in diverse skeletal muscles and cardiac muscle of transgenic mice. *Mol Cell Biol* **9**: 5058–5068.
- Zolotukhin, S, Potter, M, Zolotukhin, I, Sakai, Y, Loiler, S, Fraites, TJ Jr *et al.* (2002). Production and purification of serotype 1, 2, and 5 recombinant adeno-associated viral vectors. *Methods* **28**: 158–167.
- Zolotukhin, S, Potter, M, Hauswirth, WW, Guy, J and Muzycka, N (1996). A “humanized” green fluorescent protein cDNA adapted for high-level expression in mammalian cells. *J Virol* **7**: 4646–4654.
- Klein, RL, Meyer, EM, Peel, AL, Zolotukhin, S, Meyers, C, Muzycka, N *et al.* (1998). Neuron-specific transduction in the rat septohippocampal or nigrostriatal pathway by recombinant adeno-associated virus vectors. *Exp Neurol* **150**: 183–194.
- Brooks, SV and Faulkner, JA (1988). Contractile properties of skeletal muscles from young, adult and aged mice. *J Physiol* **404**: 71–82.
- Frimel, TN, Kapadia, F, Gaidosh, GS, Li, Y, Walter, GA and Vandenberg, K (2005). A model of muscle atrophy using cast immobilization in mice. *Muscle Nerve* **32**: 672–674.
- Petrof, BJ, Shrager, JB, Stedman, HH, Kelly, AM and Sweeney, HL (1993). Dystrophin protects the sarcolemma from stresses developed during muscle contraction. *Proc Natl Acad Sci USA* **90**: 3710–3714.